

Using heavy-ion collisions to elucidate the asymmetric equation-of-state

Sherry Yennello & Alan McIntosh

Cyclotron Institute & Department of Chemistry, Texas A&M University, College Station, TX 77845

E-mail: yennello@comp.tamu.edu

Abstract. The nuclear equation-of-state impacts a number of nuclear properties as well as astrophysical processes. The asymmetric term of the equation-of-state, which describes the behavior away from $N=Z$, has significant uncertainty. Giant resonances and nuclear masses can elucidate the asymmetry energy for cold normal-density nuclei. Heavy-ion collisions can be used to probe nuclear matter at higher temperatures and densities away from saturation density. The temperatures that are attained in these nuclear collisions are predicted to depend on the isospin asymmetry. In this work we present evidence of the asymmetry dependence of the nuclear caloric curve.

1. Introduction

The equation-of-state of any substance describes the relationship between state variables such as temperature, pressure, internal energy, composition and volume. The advent of beams of rare ions in recent years have allowed nuclear scientists to explore the equation-of-state with respect to the composition (neutron-to-proton ratio) of the nuclear material. The nuclear equation-of-state (nEOS) is important for understanding astrophysical reactions and the formation of the elements. The mass-radius relationship of neutron stars and the cooling rate of neutron stars are both dependent on the nEOS[1, 2]. The nucleus has long been modeled as a drop of liquid. As such an interesting quantity would be the specific heat of nuclear material. One particular aspect of the nucleus that needs to be taken into account is that the nuclear material is a two-component liquid, thus the composition - the neutron fraction or neutron-to-proton ratio - is important to know when determining the specific heat. In recent works [3, 4, 5] a significant dependence of the temperature on the asymmetry has been demonstrated. A quantum treatment allows one to extract densities along with the temperatures, thus enabling a map of the liquid-gas co-existence curve[6]. This manuscript will describe the progress we have made on understanding the composition dependence of the relationship between the temperature and excitation energy of nuclear material - commonly referred to as the nuclear caloric curve.

2. Experiment

The experiment was performed at Texas A&M University Cyclotron Institute using beams from the K500 superconducting cyclotron. Reactions of $^{70}\text{Zn} + ^{70}\text{Zn}$, $^{64}\text{Zn} + ^{64}\text{Zn}$ and $^{64}\text{Ni} + ^{64}\text{Ni}$ at 35 MeV/nucleon were studied with the fragments resulting from these collisions being detected in the NIMROD array[7]. NIMROD is a 4π particle detector housed inside a large



neutron detector. This enables detection of light charged particles (LCP) and intermediate mass fragments with isotopic identification up to $Z=17$ as well as detection of free neutrons. With the isotopic identification of charged particles and the measurement of free neutrons the excited quasiprojectile (Q_p) is reconstructed, so that we know its mass, charge and excitation energy. Using the isotopic information from the reconstruction the composition of the reconstructed Q_p is quantified by the m_s ,

$$m_s = (N - Z)/A.$$

For details of the experiment, see refs[8, 9, 10].

3. Nuclear Caloric Curve

The nuclear ‘‘caloric curve’’ is the relationship between the temperature of an excited nuclear system and the internal excitation energy of that system. The temperature of an excited nuclear system can be measured in various ways, using both kinetic and chemical information found in the particles emitted from a reaction. Some theoretical models have predicted that the caloric curve would be higher for more neutron-rich systems while other studies have predicted that it would be lower[11, 12, 13, 14, 15, 16]. Two previous experimental attempts have been made at detecting a composition dependence in the nuclear caloric curve [17, 18], that were unable to definitively settle this issue.

3.1. MQF Thermometer

The first thermometer we used to measure the nuclear caloric curve is the momentum quadrupole fluctuation thermometer (MQF) which is based on the kinetic information which relates fluctuations in the shape away from the ground state shape to the temperature of the excited nuclear system. Details of the method and previous uses can be found in these references [17, 19, 20] Figure 1 shows the temperature extracted versus the excitation energy of the system for five different bins in composition. As one would expect the more energy that is put into the system the higher the temperature of that system. This behavior is demonstrated for each of the composition bins. However the bins with the lowest neutron to proton composition express the highest temperatures. As more neutrons are added to the system the temperature decreases. This is systematically true across all excitation energies. One of the significant differences

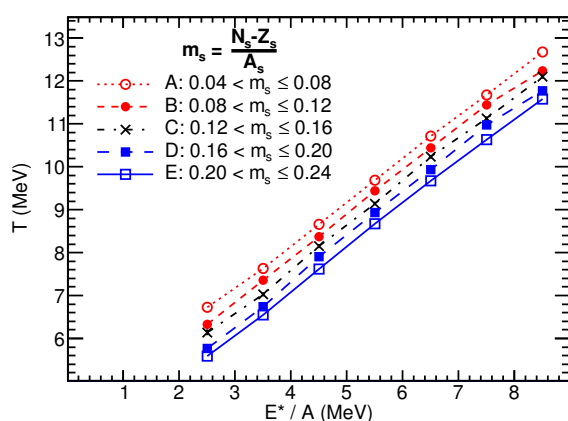


Figure 1. Temperature extracted with the MQF method as a function of excitation energy using protons for bins in m_s . ($m_s = \frac{(N-Z)}{A}$).

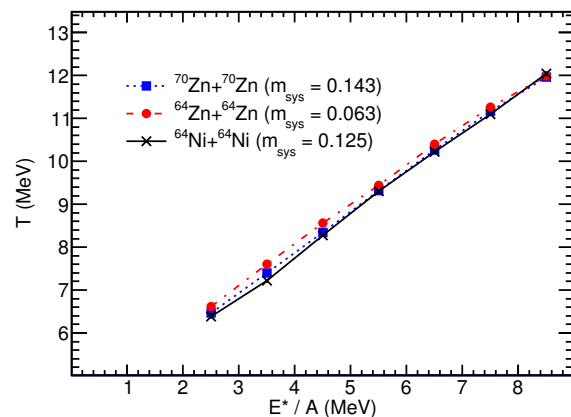


Figure 2. Temperature extracted with the MQF method as a function of excitation energy using protons from the reactions of $^{70}\text{Zn} + ^{70}\text{Zn}$, $^{64}\text{Zn} + ^{64}\text{Zn}$ and $^{64}\text{Ni} + ^{64}\text{Ni}$, ($m_s = \frac{(N-Z)}{A}$).

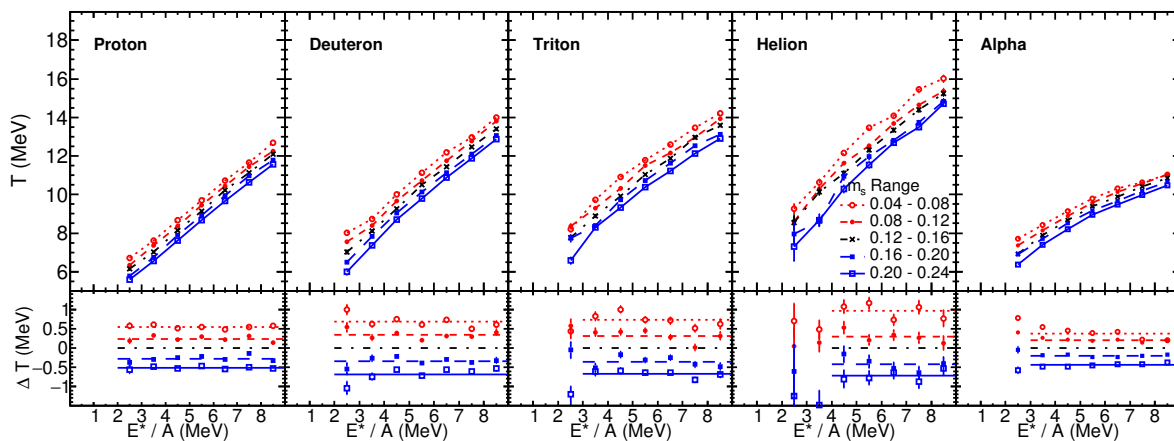


Figure 3. (Top) Temperature extracted with the Momentum Quadrupole Fluctuation method as a function of excitation energy per nucleon for light charged particles, selected on bins in asymmetry. (Bottom) Change in temperature due to a change in asymmetry as a function of excitation energy per nucleon. The middle asymmetry bin is used as the reference, ($m_s = \frac{(N-Z)}{A}$).

between the current measurement and the previous measurements is how the composition of the system was determined. In both previous measurements the composition of the system was taken as the composition of the reacting system. For the data shown in figure 1 the composition of the system was taken as the composition of the reconstructed Q_p as quantified by the m_s . Previous work has demonstrated that after the projectile interacts with the target and a hot Q_p is formed, there is a diversity in the composition of the excited Q_p [21, 22, 23] by sorting on the composition of the reconstructed Q_p the composition is more accurate and has less variation within the bin. For comparison figure 2 shows the temperature versus excitation energy for the three reacting systems with different initial compositions. As one can see the temperature rises as the excitation energy is increased just as in figure 1. However, in contrast to figure 1 the difference in the caloric curve for the three different systems is much less than when the composition was determined by the fragmenting system rather than the reacting system. The difference is still in the same direction, but the effect has been muted significantly. This analysis bridges the apparent gap between the measurement shown in figure 1 and the previous measurements where very little difference was found in the caloric curve as a function of composition.

The analysis presented in figures 1&2 was done with protons as the probe particle, but a similar analysis could be performed with other probe particles. Figure 3 shows the caloric curves for all of the light charged particles (LCP), protons, deuterons, tritons, helions, and alphas. For all of the LCP probes the temperature increases as a function of the excitation energy as one would expect. For helions the temperatures are a bit higher and for alphas a bit lower. Additionally for the alpha particles the slope of the curve is much less steep. To focus on the energy dependence of the difference the bottom panels show point by point the difference in temperature between the given m_s bin and the temperature of the central m_s bin ($m_s = 0.12-0.16$) The average across all excitation energies is shown by the horizontal lines. While the alpha particles exhibit a small energy dependence in the temperature difference the other probe particles are independent of excitation energy.

Figure 4 shows the temperature as a function of excitation energy for the various m_s bins using ${}^7\text{Li}$ and ${}^9\text{Be}$ as probe particles. While the behavior is similar to the LCP, the data shows more scatter due to limited statistics. These larger clusters also exhibit higher temperatures.

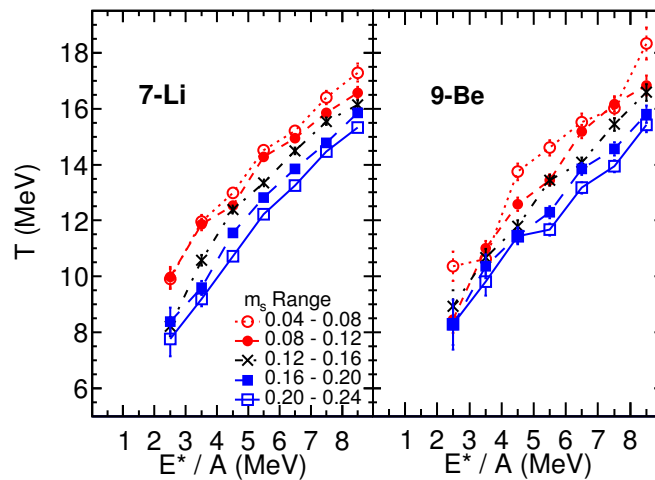


Figure 4. MQF Temperature as a function of excitation energy with ${}^7\text{Li}$ and ${}^9\text{Be}$ probes, for bins in asymmetry, ($m_s = \frac{(N-Z)}{A}$).

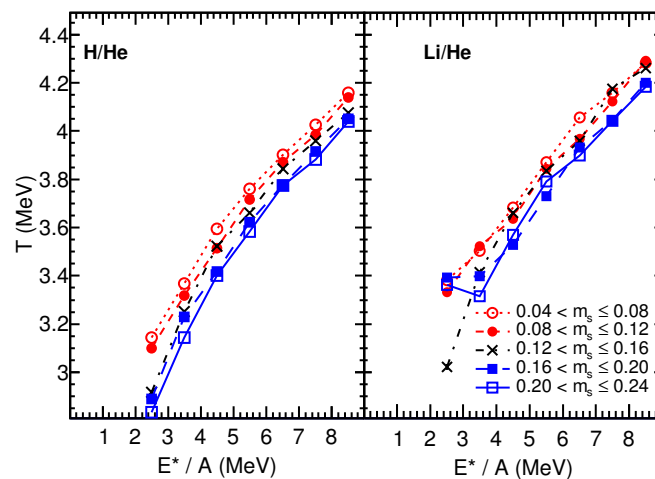


Figure 5. Temperatures calculated with the Albergo yield ratio method versus excitation energy for various bins in asymmetry, ($m_s = \frac{(N-Z)}{A}$).

This particle type dependence is similar to what was seen in previous data [17].

3.2. Chemical Thermometer

The effect of additional neutron content on the temperature expressed by an excited nuclear system as a function of excitation energy is quite clear using the MQF, which is a kinetic thermometer. Alternatively one could use the double isotope ratio or ‘‘Albergo’’ thermometer [24]. The Albergo thermometer compares the double ratios of pairs of isotopes that are different by one proton which are composed of isotopes that are different by 1 neutron. The temperatures extracted from the $\frac{p/d}{{}^3\text{He}/{}^4\text{He}}$ are shown on the left hand side of figure 5 while the temperatures extracted from the $\frac{{}^6\text{Li}/{}^7\text{Li}}{{}^3\text{He}/{}^4\text{He}}$ are shown on the right side. Again the temperature as a function of energy raises as one would expect and was seen with the MQF thermometer. The lowest m_s

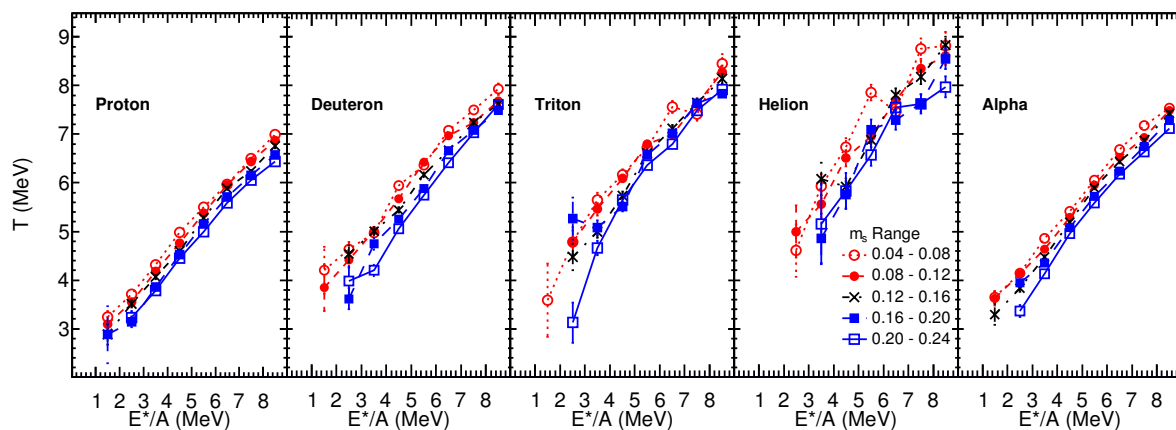


Figure 6. Slope temperatures for light charged particles versus excitation energy for bins in asymmetry, ($m_s = \frac{(N-Z)}{A}$).

bins - those with a composition closes to $N=Z$ - express the highest temperatures relative to those with more neutron content, as a function of excitation energy.

3.3. Slope Thermometer

Another method used to determine the temperature of an excited nuclear system is to measure the kinetic energy of the particles that are emitted by that system. The kinetic energy spectra can them be fit with a Boltzman distribution and a temperature can be extracted[25]. Figure 6 shows the temperatures extracted from the kinetic energy spectra of each of the light charged particle species for each of the m_s bins. Once again the temperature rises as a function of the excitation energy for all curves. The lowest m_s bin shows the highest temperature for each excitation energy bin. This is consistent across all particle types.

4. Summary

We have measured the temperature as a function of energy - or the nuclear caloric curve - for systems of various neutron - to - proton compositions. Three different thermometer methods have been used including ones based on both kinetic and chemical information. For each of the three thermometers multiple probe particles have been used. For all systems it is found that the larger the neutron content of the system the lower the temperature is for a given excitation energy. Figure 7 summaries all the data to show that as the m_s increases the temperature decreases. The top panel of figure 7 shows the magnitude of the temperature decrease as the neutron content is increased for all the probes used with the MQF thermometer. Each of the point represents the difference in the horizontal lines in figure 3 (and the equivalent difference extracted in a similar way for the ${}^7\text{Li}$ and ${}^9\text{Be}$ data shown in figure 4). The dotted lines are linear fits to the data. The middle panel shows the decrease in temperature with increasing asymmetry for the two chemical thermometers. The bottom panel of figure 7 shows the magnitude of this asymmetry dependence as extracted from the slope temperatures. While the absolute magnitude of the effect depends on the thermometer and the particular probe particle used, there is a clear linear dependence of the decrease in in the temperature with increasing asymmetry across all probes. These experimental findings are in agreement with theoretical predictions[12, 11].

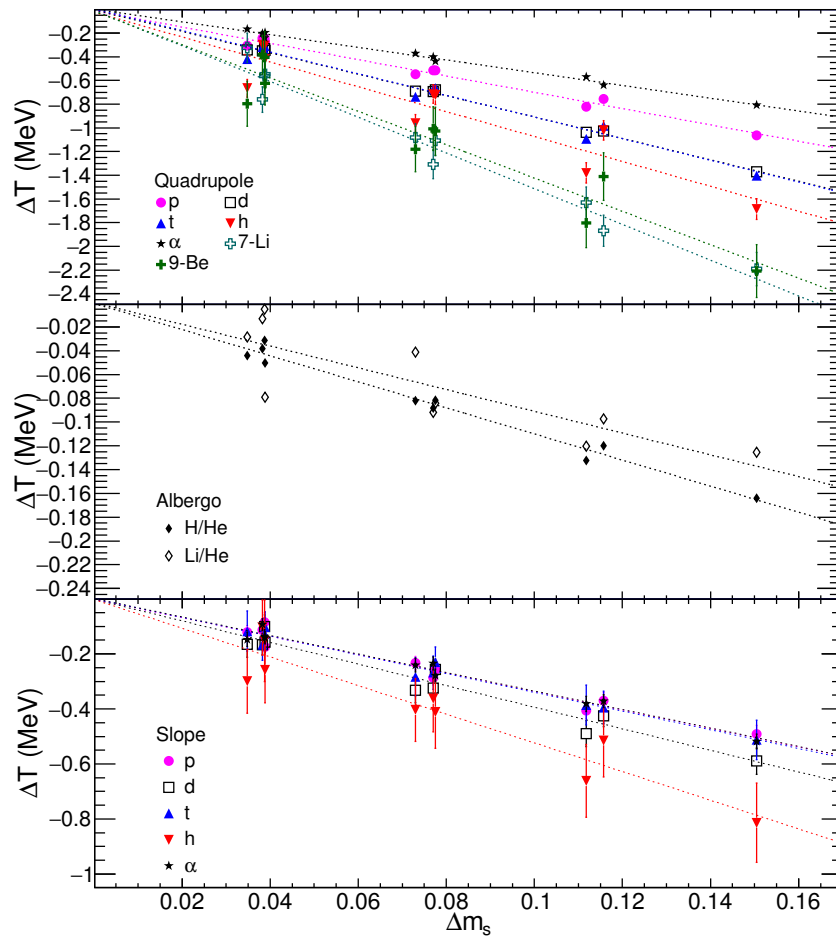


Figure 7. Change in the temperature with changing asymmetry, as determined with the MQF method (upper panel), the Albergo method (middle panel), and the slope temperature method (lower panel). The dotted lines are linear fits to the data. ($\Delta T = T_1 - T_2$; $\Delta m_s = \frac{(N_1 - Z_1)}{A_1} - \frac{(N_2 - Z_2)}{A_2}$).

Acknowledgements

This work was supported in part by the US Department of Energy under grant DE-FG02-93ER40773 and the Robert A. Welch Foundation under grant A-1266. We are indebted to the staff at the Texas A&M Cyclotron Institute for providing the high quality beams that made this work possible.

References

- [1] A.W. Steiner, Phys. Rev. C **85**, 055804 (2012)
- [2] F.J. Fattoyev, J. Piekarewicz, Phys. Rev. C **86**, 015802 (2012)
- [3] A.B. McIntosh et al., Phys. Lett. B **719**, 337 (2013)
- [4] A.B. McIntosh et al., Phys. Rev. C **87**, 034617 (2013)
- [5] A.B. McIntosh et al., EPJA **50**, 35 (2014)
- [6] J. Mabila et al., Int. J. Mod. Phys. E **22**, 1350090 (2013)
- [7] S. Wuenschel et al., Nucl. Inst. Meth. A **604**, 578 (2009)
- [8] Z. Kohley et al., Phys. Rev. C **86**, 044605 (2012)
- [9] Z. Kohley, Ph.D. thesis, Texas A&M Univ. (2010)

- [10] Z. Kohley et al., Phys. Rev. C **83**, 044601 (2011)
- [11] C. Hoel, L.G. Sobotka, R.J. Charity, Phys. Rev. C **75**, 017601 (2007)
- [12] V.M. Kolomietz, A.I. Sanzhur, S. Shlomo, S.A. Firin, Phys. Rev. C **64**, 024315 (2001)
- [13] J. Besprosvany, S. Levit, Phys. Lett. B **217**, 1 (1989)
- [14] R. Ogul, A.S. Botvina, Phys. Rev. C **66**, 051601(R) (2002)
- [15] J. Zhang et al., Phys. Rev. C **54**, 1137 (1996)
- [16] J. Su, F.S. Zhang, Phys. Rev. C **84**, 037601 (2011)
- [17] S. Wuenschel, Ph.D. thesis, Texas A&M Univ. (2009)
- [18] C. Sfienti et al., Phys. Rev. Lett. **102**, 152701 (2009)
- [19] S. Wuenschel et al., Nucl. Phys. A **843**, 1 (2010)
- [20] H. Zheng, A. Bonasera, Phys. Rev. C **86**, 027602 (2012)
- [21] D. Rowland et al., Phys. Rev. C **67**, 064602 (2003)
- [22] S. Wuenschel et al., Phys. Rev. C **79**, 061602(R) (2009)
- [23] S. Galanopoulos et al., Nucl. Phys. A **837**, 145 (2010)
- [24] S. Albergo, S. Costa, E. Costanzo, A. Rubbino, Il Nuovo Cimento **89**, 1 (1985)
- [25] D.J. Morrissey, W. Benenson, W.A. Friedman, Ann. Rev. Nucl. Part. Sci. **44**, 27 (1994)